Physicochem. Probl. Miner. Process., 61(5), 2025, 211848

http://www.journalssystem.com/ppmp

Physicochemical Problems of Mineral Processing

ISSN 1643-1049

Influence of ion concentration in water on the flotation response of pyrrhotite superstructures

L. Babedi, E. Murhula, C.E. Gibson

The Robert M. Buchan Department of Mining, Queen's University, Kingston, Ontario, Canada

Corresponding author: Babedi.lebogang@gmail.com

Abstract: This study investigates the intrinsic relationship between surface charge, redox properties, and collector interaction on determining the flotation performance of hexagonal and monoclinic pyrrhotite under deteriorating water conditions. Microflotation, UV-Vis spectrophotometry, zeta potential, and rest potential measurements were used under five different water chemistries with different ionic strengths at three different pH values (7, 9, and 11). The results indicated that although collector uptake is a function of ionic strength, flotation performance is controlled by the character of the surface species formed, which are a function of electrochemical conditions themselves. Zeta potential analysis indicated progressive double-layer compression at higher ionic strengths, particularly at alkaline pH, which contributed to enhanced collector adsorption but not necessarily improved flotation performance. Rest potential analysis indicated a transition from hydrophobic dixanthogen to surface-bound metal xanthate species as the condition became oxidative or chemically more complicated. These surface changes were amplified for monoclinic pyrrhotite, which consistently exhibited higher susceptibility to oxidation and electrochemical instability compared with hexagonal pyrrhotite. The correlation of the results indicated that flotation success is not only a function of collector uptake, but also of surface charge and redox potential compatibility to allow for the forming of stable hydrophobic layers. This study illustrates the need of including water as an additional factor in knowledge of flotation response of pyrrhotite, enabling most effective rejection in processing streams.

Keywords: pyrrhotite, rest potential, zeta potential, xanthate collector, ionic composition.

1. Introduction

Water is a critical component for achieving optimal separation of target minerals from associated gangue minerals in the flotation process. In the early years of mineral processing, water's primary role in a processing plant was seen as a transport medium, moving particles through slurries across various stages. However, over time, studies have shown that water is not merely a transport medium but also a reagent that participates in the chemical reactions that induce hydrophobicity of the target minerals. While it is well-known that selective separation of mineral constituents is facilitated using collectors, depressants, frothers, and activators (Davis et al., 1975; Wiese, 2009), while several studies research have highlighted ionic composition as an additional variable to consider for achieving optimal flotation performance.

The performance of common flotation reagents is susceptible to changes in the ionic properties of water, which can, in turn, influence subsequent interactions with particles (Manono et al., 2012, Manono et al., 2018). Dzingai et al. (2020) stated that the phenomena in both the pulp and froth phases of flotation can be affected by changes in ion-reagent-particle interactions. Due to the ongoing challenges of water scarcity and environmental concerns, mining operations have increasingly adopted closed water circuits in their process designs, emphasizing the recycling of plant water (Muzenda, 2010; Dzingai et al., 2020). However, recycled water typically contains high concentrations of ions and other residual components (Muzenda, 2010). Common contaminants in recycled water include various ions (SO_4^{2-}, Cl^-, F^-, Mg^{2+}, Ca^{2+}, Na^+, K^+) as well as residues of reagents (collectors, activators, frothers, depressants), leading to complex ionic composition (Slatter et al., 2009). While the use of recycled water has demonstrated both economic and environmental benefits, the intricate chemistry involved has

DOI: 10.37190/ppmp/211848

produced conflicting impacts on flotation performance in sulfide mineral processing plants. Studies by Cho and Laskowski (2002) and Corin et al. (2011) indicated that the presence of these ions can either hinder the flotation of certain sulfide minerals or enhance it by acting as activators. However, in the absence of well-established ion content thresholds for recycled plant water, understanding the precise impact on sulfide mineral flotation remains disjointed.

To date, an extensive body of literature illustrates how different water chemistries affect the flotation behavior of sulphide minerals (Davis et al., 1975, Craig et al., 1993, Levay et al., 2001, Cho & Laskowski, 2002, Slatter et al., 2009, Wiese, 2009, Boujounoui et al., 2015, October et al., 2019, October et al., 2021). The knowledge of ionic composition was further expanded by the work of Craig et al. (1993) and Levay et al. (2001), both stating that changes in the ionic composition destabilize bubble formation and that Ca and Mg ions can alter sulphide mineral hydrophobicity. The contrasting impact of ionic composition changes was reported by Slatter et al. (2009) stating that high ion concentrations in recycled water could influence flotation efficiency positively and negatively, depending on the mineral type and specific flotation reagents in use. The ionic strength of plant water was reported to influence the flotation response of both the target mineral and gangue mineral from platinum bearing ores from the Merensky reef (Corin et al., 2011). Manono et al. (2012) and Manono et al. (2018) demonstrated that both the type and concentration of ions, such as sulfate and chloride, present in water have notable effects on platinum ore flotation, influencing factors like recovery and selectivity between minerals. October et al. (2021) investigated the effect of ions like Ca^{2+} and Mg^{2+} on pyrrhotite bubble-particle attachment, reporting that increased ionic strength reduces attachment probability and depresses flotation performance, especially at high pH due to the formation of oxyhydroxo species that alter surface charge. Similarly, Boujounoui et al. (2015) showed that ions such as Cu^{2+} and Zn^{2+} at specific concentrations positively or negatively influence flotation based on their interaction with sulphide minerals like chalcopyrite and pyrrhotite. Their study at the Hajar Mine found that high concentrations of SO_4^{2-} enhanced recovery, while Ca^{2+} and Mg^{2+} tended to depress flotation by forming hydrophilic layers on mineral surfaces.

While extensive knowledge exists on the impacts of ionic composition variation on flotation performance, some knowledge gaps persist, requiring further investigation. One such gap is related to the impact of ionic composition on the flotation of sulphide minerals which exist in more than one polymorph (i.e. crystal structure). For example, several studies have explored the impact of ionic composition on pyrrhotite (Boujounoui et al., 2015, October et al., 2019, October et al., 2021). However, while they report critical fundamental knowledge, many of them do not present data that considers the differences in pyrrhotite structures (i.e. monoclinic and hexagonal structures). For example, the work of Multani et al. (2018) presented knowledge on the flotation behavior of the two pyrrhotite superstructures but did not extend to explore the changes in this fundamental flotation behavior as a function of ionic composition.

To fill this knowledge gap, this study uses 4 synthetic plant waters with varying concentrations of ions (Ca^{2+}, Mg^{2+}, Cl^-, Na^+ and SO_4^{2-}) to evaluate their influence on flotation performance of both hexagonal and monoclinic pyrrhotite. These responses are further explained through observation of the impact of these water chemistries on the collector adsorption, surface charge and electrochemistry of pyrrhotite superstructures across different pH levels. This fundamental understanding is critical for the optimization of Cu-Ni ores where the use of plant water is prominent and the rejection of pyrrhotite is of both economic and environmental significance.

2. Materials and methods

2.1. Samples

The hexagonal pyrrhotite sample used for this study was purchased from Ward's Natural Science, originating from the Galax Mine in Virginia, USA. Monoclinic pyrrhotite was obtained from the Clarabelle Mill feed at Vale using a hand magnet. To assure accuracy and consistency in particle size, both mineral samples were dry crushed using a stainless-steel pulverizer to get a constant size fraction between -120 µm / +75 µm.

2.2. Chemicals

Synthetic plant water solutions were prepared using a combination of reagent-grade sodium chloride ($NaCl$, 99% purity), calcium chloride ($CaCl_2$, 96% purity), and magnesium sulfate ($MgSO_4$, 99.5%

purity), all sourced from Sigma-Aldrich. Hydrochloric acid (HCl, 37% purity) and sodium hydroxide (NaOH, 98% purity), both of analytical grade, were used as pH modifiers as required. Methyl Isobutyl Carbinol (MIBC), having a purity of 99% obtained from Sigma-Aldrich was used as the frother during microflotation, while Potassium amyl xanthate (PAX) was used as the primary collector in the flotation tests, both reagents were sourced from Thermo Fisher Scientific.

2.3. Mineralogical phase identification

To confirm the mineral phases and crystallographic structures of the pyrrhotite samples, X-ray diffraction (XRD) analysis was carried out using a Malvern Panalytical Empyrean diffractometer. The instrument was operated at 45 kV and 40 mA with Cu Kα radiation. Each sample was finely ground and scanned over a 2θ range of 5–100°, ensuring a comprehensive view of the diffraction pattern. Phase identification was completed using HighScore Pro 4.9 software alongside the ICDD PDF-4+ 2021 database. Fig. 1A and 1B show the characteristic XRD spectra for hexagonal and monoclinic pyrrhotite, respectively. The hexagonal form (Fig. 1A) revealed strong peaks near 30.1°, 35.1°, 43.3°, and 55.1° 2θ, while the monoclinic form (Fig. 1B) displayed its main reflections around 30.0°, 33.1°, 43.1°, and 53.2° 2θ. These patterns are consistent with known reference data for each structure, confirming their identity. The sharp, well-defined peaks also indicate high crystallinity. Based on the pattern analysis, both samples were determined to be over 90% pure, supporting the reliability of the subsequent flotation and surface interaction studies.

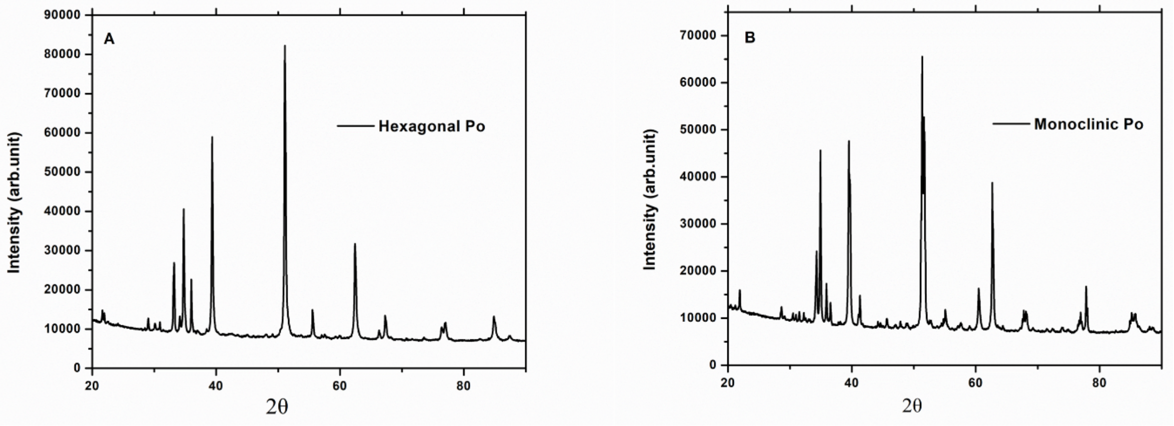

Fig. 1. XRD spectra of (A) hexagonal pyrrhotite and (B) monoclinic pyrrhotite, confirming their distinct crystallographic structures with mineral purity exceeding 90%

Additional insight into the atomic-scale structure of the two pyrrhotite types is provided in Fig. 2A and 2B, which show representative slab models generated using VESTA. The hexagonal structure (Fig. 2A) follows a NiAs-type arrangement (*P6₃/mmc*) with relatively regular Fe–S stacking and minimal long-range vacancy ordering. In contrast, the monoclinic form (Fig. 2B) exhibits distinct superstructure features arising from ordered iron vacancies along specific crystallographic planes (*C2/c*), resulting in distortions to the Fe–S framework. These structural deviations introduce undercoordinated surface sites and localised strain, which are absent or less pronounced in the hexagonal structure. Such differences are likely to influence surface reactivity and the distribution of defect sites that act as adsorption centres during collector interaction.

2.4. Synthetic plant water

Synthetic plant waters (SPWs) were prepared to replicate process water conditions, by including variable quantities of Na^+, Ca^{2+}, Mg^{2+}, Cl^-, and SO_4^{2-} ions at concentrations in line with the work of October et al. (2021). These concentrations were originally adopted by October et al. (2021), who based their selection on Wiese et al. (2005), where such ionic levels were measured in process water from Merensky reef concentrators in South Africa, reflecting realistic operating conditions in PGM flotation circuits. Stock solutions of 1 M sodium chloride (NaCl), calcium chloride ($CaCl_2$), and magnesium sulfate ($MgSO_4$) were used to achieve target ion concentrations by diluting required quantities of each

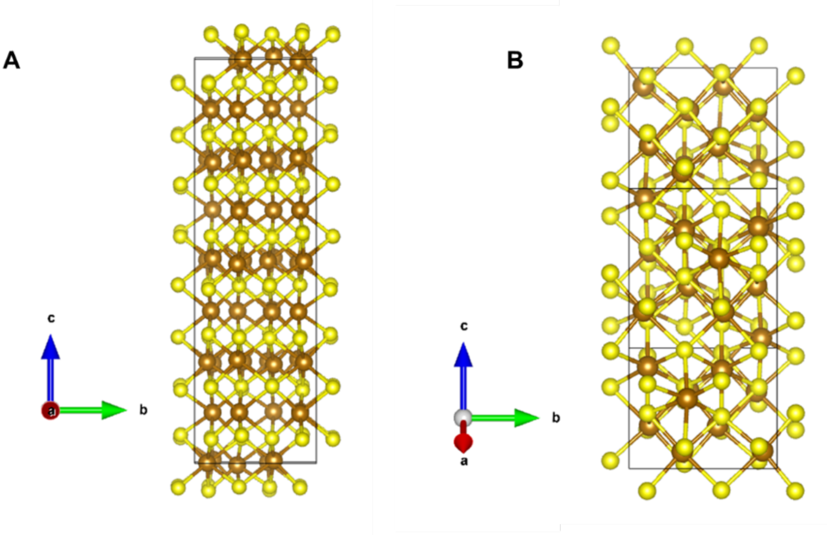

Fig 2. VESTA-generated slabs of pyrrhotite viewed along [100]. (A) Hexagonal structure with regular Fe–S stacking. (B) Monoclinic structure showing vacancy ordering and lattice distortion

stock solution in 1 liter of deionized water. For each ion concentration, 100 mL of the corresponding 1 M stock solution was made, and aliquots were taken to achieve the final concentrations in 1 L of synthetic plant water. To have a consistent ionic profile, the pH was modified with 0.1 M hydrochloric acid (HCl) and 0.1 M sodium hydroxide (NaOH); HCl and NaOH solutions were prepared using each type of synthetic water. This allowed pH modifications without the introduction of extra ions or modification of the synthetic water composition. Table 1 displays the ionic concentrations in each SPW, with Cl^- and SO_4^{2-} values obtained from the additions of NaCl, $CaCl_2$, and $MgSO_4$.

Table 1. Concentration of specific ions in prepared synthetic plant waters (SPWs)

Water Type	**Na^+ (mg/L)**	**Ca^{2+} (mg/L)**	**Mg^{2+} (mg/L)**	**Cl^- (mg/L)**	**SO_4^{2-} (mg/L)**
Ultrapure	-	-	-	-	-
SPW1	300	150	90	730.5	354
SPW2	800	400	240	1872	944
SPW3	1200	600	360	2808	1416
SPW4	2000	1000	600	4950	2360

2.5. Microflotation

Microflotation experiments were conducted to assess the flotation behavior of hexagonal and monoclinic pyrrhotite under varying water chemistries and pH levels (7, 9, and 11). These tests aimed to evaluate the influence of pH and ionic strength on flotation recovery under controlled laboratory conditions. Each test was carried out in a custom made 60 mL cylindrical glass flotation cell (Fig. 3) containing 40 mL of synthetic plant water (SPW) adjusted to the target pH using dilute NaOH or HCl. A 1.0 g sample of pyrrhotite, with a particle size fraction between -120 µm and +75 µm, was added to the cell and conditioned by magnetic stirring at 1300 rpm for 5 minutes. Potassium amyl xanthate (PAX) was added at a concentration of 50 mg/L as a collector, and Methyl Isobutyl Carbinol (MIBC) was added at 80 mg/L as a frother midway through conditioning (at 2.5 minutes). Air was introduced at a flow rate of 10 mL/min to initiate flotation, which proceeded for 4 minutes. Froth was collected continuously throughout the test. After flotation, both concentrate and tailings were filtered, oven-dried at 60°C for 24 hours and weighed to determine the mass recovery of pyrrhotite. All tests were performed in triplicate across each pH level and SPW condition to ensure reproducibility and statistical confidence. Results were used to evaluate the interaction between pyrrhotite structure, pH, and ionic composition in determining flotation response.

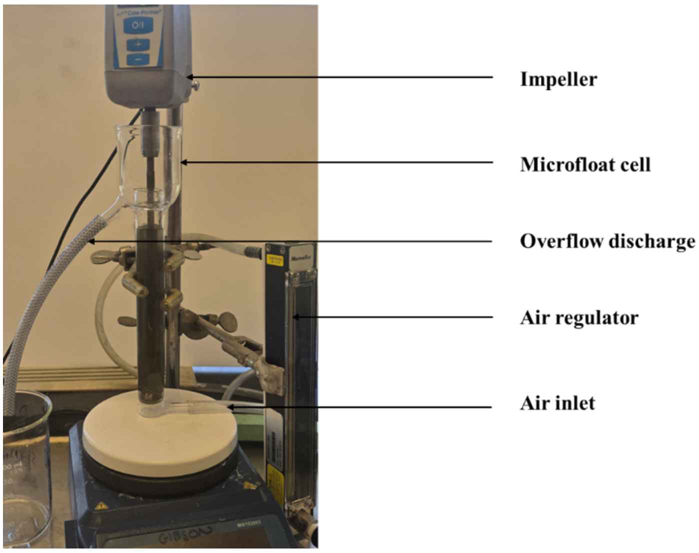

Fig. 3. Microflotation cell setup used for flotation testing of pyrrhotite samples

2.6. Collector adsorption

The impact of ionic composition on collector adsorption onto pyrrhotite superstructure surfaces was assessed using a UV-Vis spectrophotometer. A 0.1 M potassium amyl xanthate (PAX) solution was prepared and diluted to create six solutions with concentrations ranging from 10 mg/L to 70 mg/L in 100 mL of deionized (DI) water to use as calibration standards (Fig. 4). Each solution was mixed for 5 minutes, and absorbance was recorded to produce a calibration curve for PAX concentrations. For the mineral adsorption experiments, 1 g of pyrrhotite sample was placed in a 100 mL flask, and 40 mL of the selected synthetic water type with different pH was added. A concentration of 50 mg/L of 0.1 M PAX solution was introduced, followed by mixing for 5 minutes. Upon completion of mixing, the slurry was allowed to settle and filtered, and the supernatant was collected for further adsorption analysis. The absorbance spectra of the filtrate were then used to quantify the amount of collector adsorbed onto the pyrrhotite surface as a function of ionic composition and pyrrhotite type. The adsorption amount (Q) was calculated using the following formula:

$$Q = \frac{(C_1 - C_2)\cdot V}{W} \tag{1}$$

where Q represents the amount of collector adsorbed (mmol/g), where C_1 and C_2 are the collector concentrations before and after the adsorption measured in mmol/L. V shows the volume (L) used during the tests, while W represents the mass (g) of the sample.

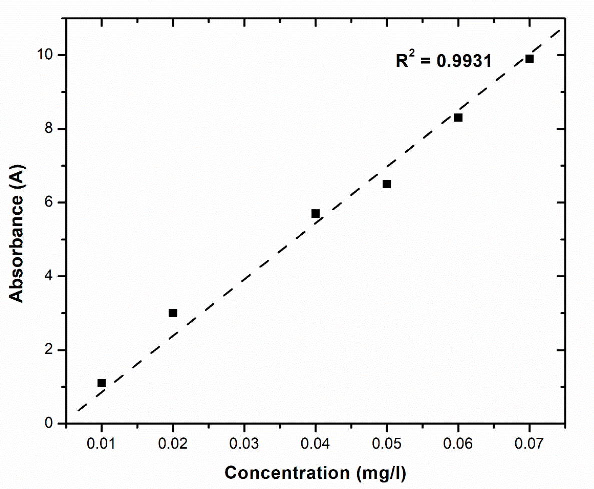

Fig. 4. Calibration curve for collector (PAX) concentration showing linear relationship between absorbance and concentration (R^2 = 0.9931)

2.7. Zeta potential

Zeta potential measurements were performed to assess the influence of ionic composition on charge reversal and collector adsorption under alkaline conditions, using a Malvern Zetasizer Nano ZS instrument. Measurements were obtained by converting electrophoretic mobility to zeta potential via the Smoluchowski equation. The different SPW were used as the background electrolyte at varying pH values ranging between 6 and 12. For each test, the pyrrhotite sample used was first pulverized to a top size of less than 25 µm. A sub-sample of 0.01 g was introduced into a 15 mL test vial, to which 15 mL of the chosen SPW and 50 mg/L of PAX were added. The mixture was mixed for 1 minute and thereafter conditioned for 5 minutes. A 2 mL aliquot of the conditioned suspension was removed and transferred to the electrophoretic cell for measurement. Electrokinetic studies were performed under varying pH levels to establish the surface charge in the presence of collector, serving as an indicator of surface behavior in different water chemistries. All experiments were conducted under room temperature conditions. The zeta potential data reflects an average of three measurements, with error bars denoting the standard error.

2.8. Rest potential

Electrochemical rest potential measurements were conducted using a Gamry Instruments Reference 600 Potentiostat/Galvanostat to assess the impact of ionic composition on pyrrhotite in the presence of a collector. The setup used a three-electrode system consisting of a reference Ag/AgCl electrode, a counter platinum electrode, and a pyrrhotite working electrode. Each pyrrhotite electrode was polished with 600-grit silicon carbide paper, followed by alumina powders of progressively smaller particle sizes (1 µm, 0.3 µm, and 0.05 µm) to expose a clean surface prior to each measurement. The electrodes were washed with deionized water and dried before immersion. Measurements were performed in a 40 mL solution of the chosen synthetic plant water (SPW) serving as the electrolyte. A 0.1 M potassium amyl xanthate (PAX) solution was prepared daily in deionized water, with 50 mg/L of PAX used for each measurement. The measurement was conducted for a total of 600 s, with the collector added at 300 s. The results were analyzed using Gamry Echem Analyst software and calibrated to the Standard Hydrogen Electrode (SHE) scale. The electrochemical response of each pyrrhotite sample was evaluated in triplicate for each SPW, with the electrode surface polished prior to each measurement to ensure precision and reproducibility.

3. Results and discussion

3.1. Influence of ionic composition on the flotation response and collector adsorption of pyrrhotite superstructures under different conditions

The degree and species of collector adsorbed on mineral surfaces largely determines the selective recovery of sulphide minerals during flotation. Several studies have shown that variation in the ionic strength of processing water as a function of changing ion content, reagent residues and mineral oxidation products can significantly influence collector adsorption and flotation performance (Corin et al., 2011; Manono et al., 2012; Muzinda and Schreithofer, 2018). The influence of ionic composition on surface-reagent interactions within pyrrhotite superstructures is discussed in this section alongside collector adsorption. Figs. 5a and 5b present under varying ionic strength and pH levels the flotation characteristics of pyrrhotite polymorphs.

Fig. 5a shows consistent flotation recovery of hexagonal pyrrhotite at pH 7 and 9, with recoveries above 70% and 65%, respectively. A slight decline occurred from DI water to SPW4, indicating that hexagonal pyrrhotite remained chemically active and interacted with the collector even under ion-enriched conditions. At pH 11, recovery dropped sharply to below 10% across all waters, confirming that excessive alkalinity inhibits hydrophobicity regardless of chemistry. By contrast, Fig. 5b shows monoclinic pyrrhotite was more sensitive to both pH and water composition. Recoveries in DI water were ~48% at pH 7, but decreased markedly in SPW2 and SPW3 with rising ionic concentration, falling below 10% at pH 9 in SPW3. This indicates flotation was influenced not only by ionic strength but also specific ion composition. At pH 11, flotation was minimal across both structures. Thus, the flotation of pyrrhotite superstructures was strongly controlled by variations in pH and ionic conditions.

In many cases, the quantity of collector adsorbed is directly related to flotation performance, since increased surface covering by hydrophobic species improves particle-bubble interaction (October et al., 2021). Consequently, to further evaluate the mechanisms driving the micro-flotation results, UV-Vis spectral data were acquired to measure the quantity of collector adsorbed on both hexagonal and monoclinic pyrrhotite surfaces. Fig. 6a and 6b shows the representative UV-Vis spectra for collector absorbed after conditioning with both hexagonal and monoclinic pyrrhotite samples under different conditions.

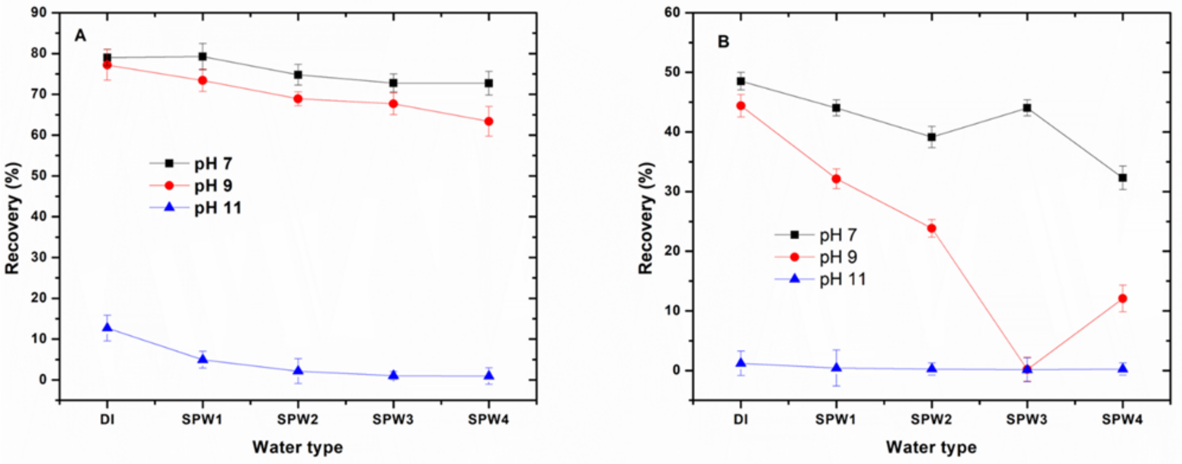

Fig. 5. The flotation recovery of hexagonal (A) and monoclinic (B) Po under different ionic composition and pH levels

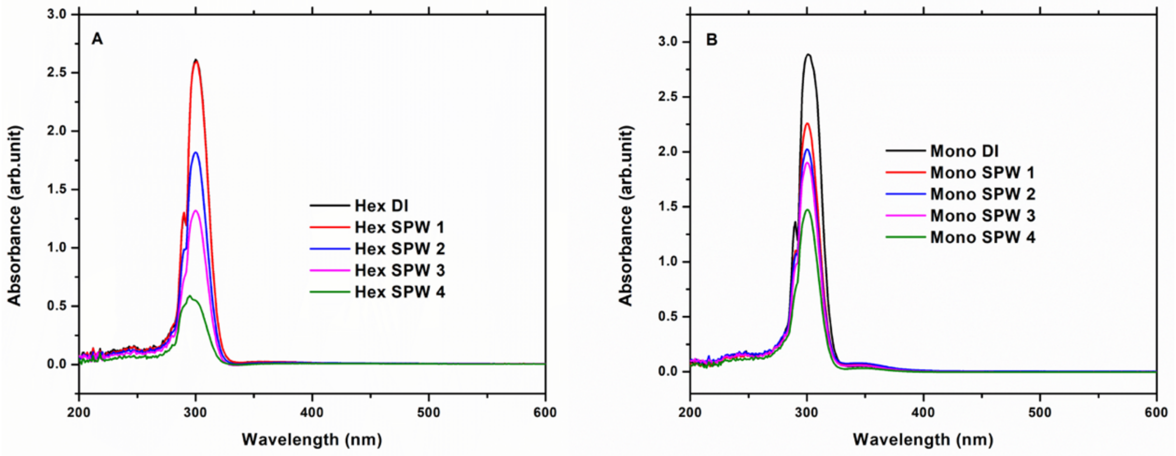

Fig. 6. UV-vis spectra of the supernatant from conditioning of hexagonal at pH 7 (A) and monoclinic Po at pH 11 (B)

Fig. 7 shows the quantity of collector adsorbed onto hexagonal pyrrhotite with different water types and pH levels. Collector adsorption typically increases with ionic strength across all pH levels, reaching its peak in SPW4. The maximum adsorption occurred at pH 7 and pH 9 in SPW4, exceeding 4 mmol/g. This suggests that, in the presence of ions, both mildly acidic and highly alkaline conditions allow the hexagonal form to remain suitable for collector attachment. Such behaviour is likely because under these conditions, hexagonal pyrrhotite retains its higher electrochemical stability and lower tendency to form passivating oxidation products hence more active sites for collector interaction. Fig. 7 for monoclinic pyrrhotite showed a similar tendency; collector adsorption increased with ionic strength, with SPW3 and SPW4 showing the maximum absorption across all pH levels. Additionally, in DI to SPW4 at pH 11, adsorption on hexagonal pyrrhotite was significantly higher than on the monoclinic form, indicating reduced collector uptake in the latter under these conditions. demonstrating that collector absorption occurred under alkaline conditions, even when flotation recovery was reduced in ion-rich environments.

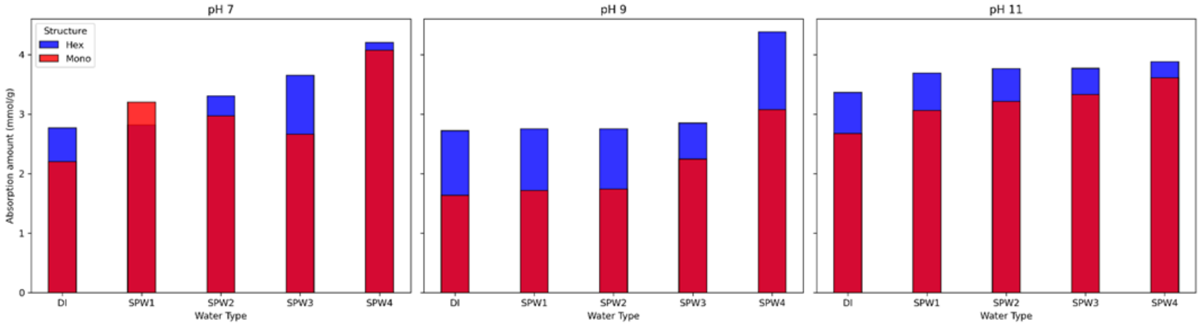

Fig. 7. Variation in the amount of collector absorbed on hexagonal (A) and monoclinic (B) Po as a function of changing ionic strength and pH

The variation in collector adsorption did not directly correspond with flotation recoveries in Figs. 5a and 5b. Although adsorption increased with ionic strength for both pyrrhotite polymorphs, recoveries diminished, particularly for monoclinic pyrrhotite. Recovery was also low at pH 11 in SPW4 for both structures despite high collector uptake. This shows that collector adsorption alone is not sufficient to ensure flotation, as adsorption can occur onto oxidized or hydrophilic sites that do not promote bubble attachment.

Monoclinic pyrrhotite is especially sensitive to surface passivation and ion competition. Multani et al. (2018) showed its tendency to form dixanthogen during controlled oxidation at low dosages, which can give the appearance of high adsorption without generating stable hydrophobicity. Our results indicate that, at pH 11 in SPW4, adsorption was high, yet recovery remained suppressed, consistent with the formation of $Fe(OH)_3$ and FeOOH films that block attachment sites (Belzile et al., 2004; Becker et al., 2010). In such cases, collector molecules are consumed on oxidized surfaces but do not translate into effective flotation.

Hexagonal pyrrhotite showed better resistance to ionic stress, maintaining recovery at pH 7 and 9 despite modest adsorption. This agrees with October et al. (2021), who reported that high ionic strength compressed the electrical double layer, improving bubble–particle attachment even when adsorption was limited. The sharp decline at pH 11, however, indicates that both polymorphs eventually became dominated by hydrophilic hydroxide species, similar to observations by Musuku and Dahl (2022), who reported stronger oxidation in recycled waters under alkaline conditions.

Ion-specific effects further explain the observed contradiction. Corin et al. (2011) and Manono et al. (2012, 2016) showed that calcium and magnesium interact with mineral surfaces and collectors, altering charge and froth behavior. Calcium in particular co-precipitates with sulfate at high pH, forming insoluble surface complexes that hinder hydrophobic layer formation despite measurable adsorption (Kirjavainen et al., 2002; October et al., 2021). Thus, the high adsorption measured under elevated ionic content does not necessarily represent functional hydrophobicity, since a large fraction of the collector is immobilized in inactive surface complexes.

Taken together, the discrepancies between adsorption and recovery reflect that flotation is controlled not only by the extent of collector uptake but also by the nature of adsorption sites, surface oxidation, and ion-driven passivation. These processes explain why high collector adsorption, particularly under high ionic strength and alkaline conditions, coincides with lower flotation recovery.

3.2. Effect of changing ionic composition on the surface charge of pyrrhotite superstructures

The magnitude and polarity of zeta potential are determined by the structure of the electrical double layer at the mineral-solution interface, significantly affected by pH and ionic content (Manono et al., 2016; Corin et al., 2011). Increasing ionic strength compresses the double layer, thereby diminishing electrostatic repulsion and possibly improving particle-bubble attachment, despite a reduction in collector adsorption (October et al., 2021; Becker et al., 2010). Furthermore, variations in surface charge often indicate more general changes in surface chemistry that is, the formation of hydrophilic oxidation products like $Fe(OH)_3$ or sulfate-containing complexes that might weaken the link between collector presence and flotation performance (Belzile et al., 2004; Muzinda and Schreithofer, 2018). Zeta potential is thus a useful instrument for understanding the electrokinetic conditions affecting flotation in pyrrhotite systems. Fig. 8 shows the average zeta potential values for both hexagonal and monoclinic pyrrhotite, measured in deionized water and four synthetic plant waters (SPW1-SPW4) at pH levels 7, 9, and 11, all in the presence of a collector.

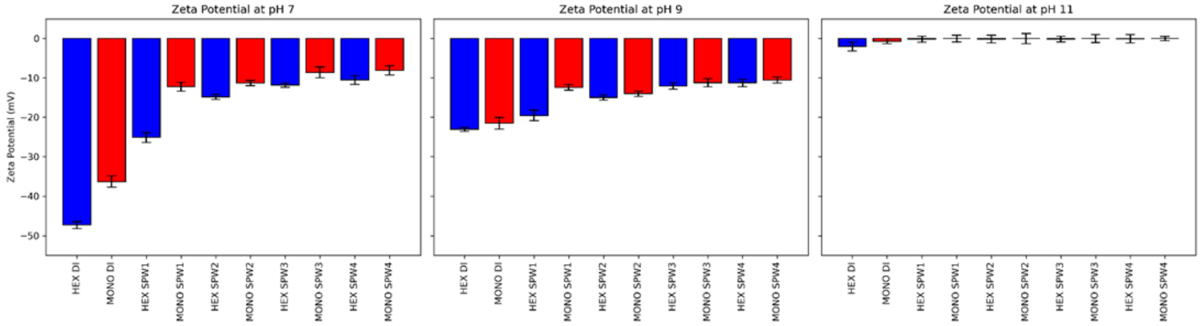

Fig. 8. Zeta potential of hexagonal and monoclinic pyrrhotite measured across varying pH levels and water chemistries after collector addition

Fig. 8 shows zeta potential variations for hexagonal and monoclinic pyrrhotite at pH 7, 9, and 11 across water types from DI to SPW4. At pH 7, both polymorphs had the most negative values in DI water, becoming progressively less negative from SPW1 to SPW4. Hexagonal pyrrhotite ranged from about −47 mV in DI to −10 mV in SPW4, while monoclinic followed a similar trend with slightly less negative values. At pH 9, surface potentials again decreased with increasing ionic concentration, with monoclinic consistently less negative. At pH 11, both polymorphs approached zero in SPW3 and SPW4, and some monoclinic samples were slightly positive. Overall, the data show a consistent decline in surface charge with rising ionic strength.

The observed trend of declining zeta potential magnitude with increasing ionic strength confirms the main influence of ionic composition in controlling the electrical double layer at the mineral-solution interface. The zeta potential, found by Salopek et al. (1992), is influenced by the thickness of the diffuse layer and the properties of adsorbed ions; it reflects the potential at the slipping plane. In solutions with high ionic strength, divalent ions like Ca^{2+} and Mg^{2+} compress the double layer and decrease surface potential, as evidenced by the change towards near-neutral zeta values found in SPW3 and SPW4 for both pyrrhotite structures.

The intrinsic structural and surface chemical differences between hexagonal and monoclinic pyrrhotite were further shown by variations in zeta potential between these polymorphs. Particularly under neutral conditions, these structural features could improve the charge density on the hexagonal surface. On the other hand, the zeta potential difference between the two forms either inverted or was reduced at higher ionic strength and alkaline pH. Especially at pH 11, both types of pyrrhotite showed either almost zero or slightly positive zeta potentials in SPW3 and SPW4. This trend shows that by effectively reducing surface charge, the main influence of ionic composition, mostly the presence of Ca^{2+} and SO_4^{2-} overcomes structural variations. October et al. (2021) noted similar behavior in galena and chalcopyrite flotation systems, observing that high ionic load results in double layer compression, which improves bubble–particle contact despite minor variations in collector uptake, suggesting a decoupling of surface charge and adsorption capacity.

The low zeta potential under these conditions correlated to a process in which particle suspensions destabilize, promoting aggregation and potentially improving flotation through hydrophobic bridging mechanisms; however, this effect may differ between polymorphs due to varying oxidation rates (Becker et al., 2010; Manono et al., 2016). However, zeta potential changes alone do not definitively forecast flotation results, as shown by Salopek et al. (1992), who stated that zeta potential represents the combined effect of several interfacial processes rather than an isolated interaction. In relation to the present study, both pyrrhotite polymorphs exhibited significant collector adsorption under specific conditions without a corresponding increase in flotation recovery. This indicates that changes in zeta potential signifies not just ion-induced double layer occurrences but also fundamental modifications in surface speciation, including the formation of oxidized or hydroxylated layers. Muzinda and Schreithofer (2018) observed that breakdown products from collectors and accumulated ions in recycled water can alter surface chemistry in ways not obvious from bulk adsorption data.

The zeta potential results confirm the intricate relationship between mineral structure, solution chemistry, and reagent interaction. The reduction of surface charge magnitude with increasing ionic strength is a consistent trend; however, its impact on flotation efficiency must be recognized in relation to oxidation factors, surface speciation, and the intricate role of multivalent ions in electrostatic and chemical adsorption mechanisms. This electrokinetic perspective, in conjunction with collector adsorption and recovery data, offers an understanding of the factors influencing pyrrhotite flotation performance under changing water quality conditions.

3.3. Electrochemical response of pyrrhotite superstructures under degrading water quality

This section examines the electrochemical response of pyrrhotite superstructures, with and without a collector, across increasingly degraded water chemistries and varying pH. Previous studies (Buswell and Nicol, 2002; Cheng, 1993; Khan and Kelebek, 2004; Tadie et al., 2015) have shown that rest potential values reflect whether dixanthogen or metal xanthate species dominate, and that these values are influenced by pH, ionic composition, and surface oxidation states. These parameters play an important role in defining the redox behaviour of the mineral–solution interface. In this context, we assess how the electrochemical stability of hexagonal and monoclinic pyrrhotite varies with increasing ionic strength and alkalinity, and we infer how such changes influence their flotation response, and the nature of surface species formed during processing. Fig. 9 presents the rest potential of hexagonal and monoclinic pyrrhotite in the absence of collector across water types and pH conditions.

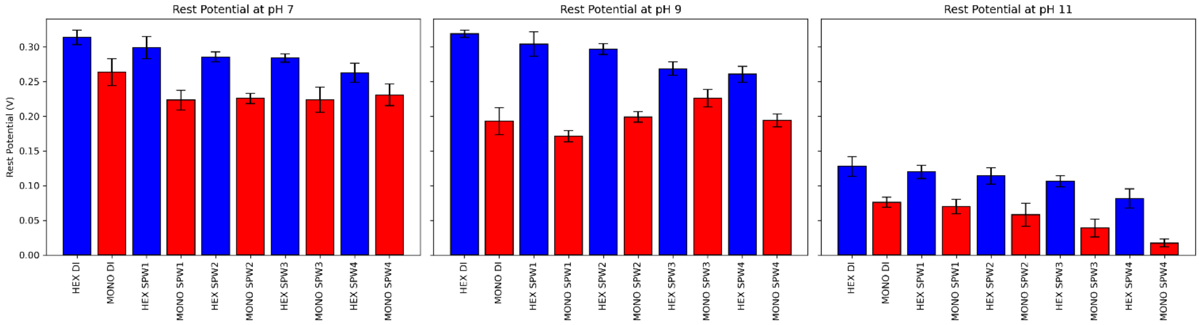

Fig. 9. Rest potential measurements of hexagonal and monoclinic pyrrhotite in the absence of collector across different ionic composition and pH

The data show a consistent decline in rest potential with increasing pH and ionic strength. The lowest values are observed at pH 11 in SPW4, where monoclinic pyrrhotite drops below 0.06 V. Conversely, the highest potentials occur at pH 7 in DI water, exceeding 0.30 V for both structures. Across all conditions, hexagonal pyrrhotite maintains higher rest potentials than monoclinic, suggesting enhanced electrochemical stability. This behaviour reflects a progressive loss in surface nobility as ionic composition becomes more complex and alkaline. High rest potentials, such as those observed in DI water at pH 7, point to a relatively passive surface with reduced redox activity, while lower potentials correspond to more reactive, oxidising conditions. These trends are consistent with studies showing that decreasing rest potential is linked to increased surface oxidation and the formation of hydrophilic layers, such as ferric hydroxide, which are known to hinder collector adsorption and reduce flotation performance (Buswell and Nicol, 2002; Cheng, 1993; Belzile et al., 2004).

The sharper drop in rest potential observed for monoclinic pyrrhotite aligns with its greater structural disorder and Fe-deficient composition, both of which are associated with increased oxidative dissolution (Multani et al., 2018; Becker et al., 2010). In more ion-rich waters (SPW3 and SPW4), the presence of ions such as Ca^{2+}, Mg^{2+} and SO_4^{2-} may further destabilize surface redox conditions by inhibiting passive layer formation and promoting alternate surface reactions (Ekmekçi et al., 2010; Manono et al., 2016). These rest potential trends under collectorless conditions provide a clear framework for understanding how water composition controls the formation of surface species like dixanthogen or metal xanthates when collectors are introduced. Fig. 10 displays the rest potential values for both mineral structures in the presence of xanthate collector.

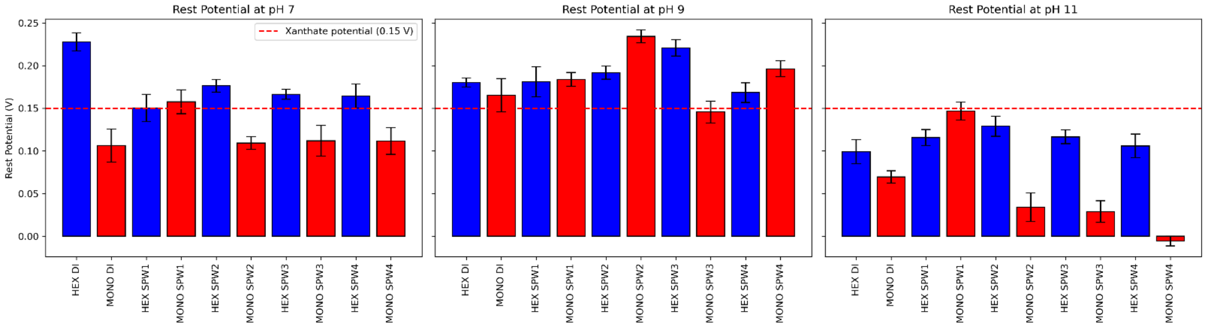

Fig. 10. Rest potential measurements of hexagonal and monoclinic pyrrhotite in the presence of xanthate collector

At pH 7 (for hexagonal pyrrhotite) and pH 9 (for both structures) in DI water and SPW1, rest potentials remain above 0.15 V, a range generally associated with the oxidation of xanthate to form hydrophobic dixanthogen layers (Buswell and Nicol, 2002). As pH rises to 11 and ionic strength increases, particularly in SPW3 and SPW4, rest potential values for monoclinic pyrrhotite and, to a lesser extent, hexagonal pyrrhotite, drop below this threshold. The decline suggests a transition from dixanthogen formation to less stable metal xanthate species as the dominant surface product (Cheng, 1993; Khan and Kelebek, 2004). While both structures are affected, monoclinic pyrrhotite exhibits a greater sensitivity, with steeper drops in rest potential under complex water chemistries. Hexagonal pyrrhotite retains a more noble electrochemical character across all conditions, often remaining close to or above the 0.15 V threshold, suggesting it provides a more stable platform for dixanthogen formation.

This drop in rest potential is likely the result of both redox imbalance and compression of the electrical double layer. Ca^{2+} and SO_4^{2-} are known to interfere with the oxidation of xanthate and the formation of dixanthogen species (Ekmekçi et al., 2010; Manono et al., 2016), while also promoting surface precipitation of iron oxides or sulfates, which inhibit electron transfer. Such effects have been linked to reduced xanthate adsorption efficiency and increased surface hydrophilicity (Belzile et al., 2004). The distinction between the two superstructures is again evident. Hexagonal pyrrhotite consistently maintains higher rest potentials, indicating a relatively stable surface environment that favours the formation of hydrophobic collector products. In contrast, monoclinic pyrrhotite is more prone to oxidation and surface transformation. Prior studies have identified the formation of $Fe(OH)_3$ and $FeSO_4$ as oxidation products on monoclinic surfaces under similar conditions (Cheng, 1993; October et al., 2021). These species are known to passivate the surface and prevent the formation of hydrophobic layers, explaining the sharp decline in rest potential and its impact on flotation chemistry. The observed transition from dixanthogen to metal xanthate dominance under increasingly alkaline and ionic conditions points to a clear electrochemical pathway that reflects the surface reactivity of each structure.

Taken together, these electrochemical measurements reinforce the notion that pyrrhotite flotation response is tightly controlled by ionic composition and the semiconducting properties of the mineral surface. As the rest potential declines with increasing ionic complexity and alkalinity, the dominant surface species shifts from hydrophobic dixanthogen to less stable metal xanthates. These findings form the basis for interpreting flotation performance under realistic process water conditions and for tailoring reagent strategies to specific mineral structures.

3.4. Interlink between zeta potential and collector adsorption on pyrrhotite surfaces

In sulphide flotation systems where redox reactions dominate, surface charge plays a central role in regulating collector attachment. This charge, indicated by zeta potential, influences the thickness of the electrical double layer and the adsorption of anionic collectors such as xanthates. Sections 3.1 and 3.2 examined how changes in pH and ionic composition impact zeta potential and collector adsorption on monoclinic and hexagonal pyrrhotite. The results showed clear differences between the two structures, highlighting that variations in ionic composition alter electrostatic conditions, which in turn affect the formation and stability of surface species. These observations align with earlier studies (Laskowski, 2013; Hodgson and Agar, 1989), which linked surface potential to collector adsorption efficiency and ultimately flotation response. The relationship between zeta potential after collector addition and the amount of collector adsorbed following conditioning is summarised in Fig. 11.

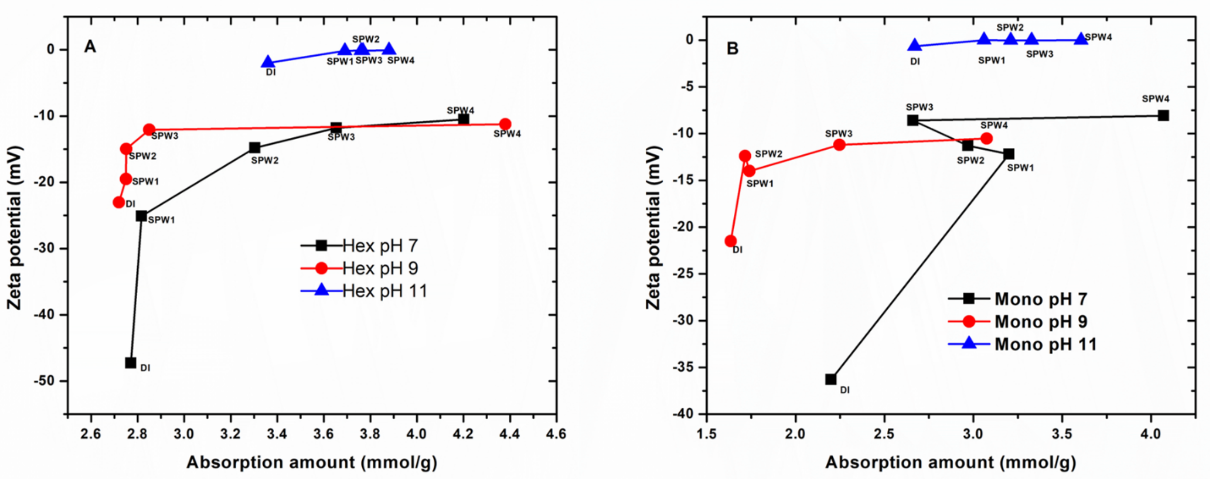

Fig. 11. The relationship between zeta potential and amount of collector absorbed by both hexagonal (A) and monoclinic (B) pyrrhotite under varying pH and ionic composition

Fig. 11 shows that the zeta potential becomes less negative as ionic strength increases from deionized water to SPW4, a trend attributed to electrical double-layer compression. However, the extent of collector adsorption differs markedly between the two structures, indicating that zeta potential alone does not sufficiently explain collector uptake, particularly for monoclinic pyrrhotite, which deviates in electrostatic behaviour.

Hexagonal pyrrhotite displayed a clear positive correlation between reduced negative zeta potential and increased collector adsorption. This is consistent with findings by Hodgson and Agar (1989), who showed that collector adsorption on pyrrhotite is primarily driven by the physisorption of dixanthogen on oxidised Fe(III) sites, rather than direct xanthate chemisorption. As the surface charge becomes less negative, likely due to Ca^{2+} and Mg^{2+} adsorption, oxidised Fe(III) species promote dixanthogen formation, enhancing collector uptake. Moreover, elevated Ca^{2+} concentrations may shift redox potential, stabilising oxidised surface species and favouring dixanthogen formation. This mechanism aligns with the higher collector adsorption observed for hexagonal pyrrhotite in SPW3 and SPW4 at all pH levels.

In contrast, monoclinic pyrrhotite exhibited lower and inconsistent collector adsorption despite similar zeta potential changes. Its structural defects and higher distortion increase its susceptibility to surface oxidation, promoting hydrophilic layer formation such as $Fe(OH)_3$ and sulphoxy precipitates, which inhibit xanthate adsorption. Calcium is known to adsorb on sulphide surfaces via multi-site coordination without proton exchange (Moignard et al., 1977), leading to surface passivation that interferes with redox transitions essential for dixanthogen production. This is evident at pH 11, where both pyrrhotite forms approach neutral zeta potential, yet only hexagonal pyrrhotite shows increased collector adsorption. Monoclinic pyrrhotite, by contrast, remains inhibited, likely due to discontinuous oxidation pathways and Fe(III) site deactivation. Additional surface coverage by $Ca(OH)^+$ and SO_4^{2-} may also hinder collector access. Voltammetric data from Hodgson and Agar (1989) further support that Ca^{2+} competes with xanthate for pyrrhotite surface sites, especially under conditions favouring sulphoxy species. This competitive adsorption likely contributes to the plateau in collector uptake observed for monoclinic pyrrhotite, despite surface charge conditions that might appear electrostatically favourable.

These results demonstrate that surface charge alone cannot account for collector behaviour. In monoclinic pyrrhotite, structural features and surface terminations likely facilitate Ca^{2+} adsorption without fully excluding xanthate, implying ion-specific surface interactions. This may involve partial ion exchange processes that reduce surface charge, as described by Moignard et al. (1977), without entirely blocking collector-accessible sites. Additionally, in high-ionic-strength media, disruption of interfacial water layers by divalent cations may further influence collector attachment and bubble-particle interactions. Together, these observations highlight that the electrochemical environment interacts with crystal structure to regulate collector response. The distinct behaviour of hexagonal and monoclinic pyrrhotite underlines the need to interpret zeta potential in the context of structural controls and site-specific chemistry, not merely electrostatics.

3.5. Correlation between electrochemical and flotation responses of pyrrhotite superstructures under varying conditions

The control of collector interaction and, consequently, flotation performance depends on the electrochemical conditions at the mineral-solution interface. This section attempts to demonstrate a direct correlation between the flotation response of hexagonal and monoclinic pyrrhotite and the corresponding rest potentials after collector addition investigated in Section 4.3. Figs. 12a and 12b illustrate the relationship between rest potential and flotation recovery for hexagonal and monoclinic pyrrhotite, respectively, across three pH conditions emphasizing the interaction of electrochemical state, mineral structure, and pH on flotation results.

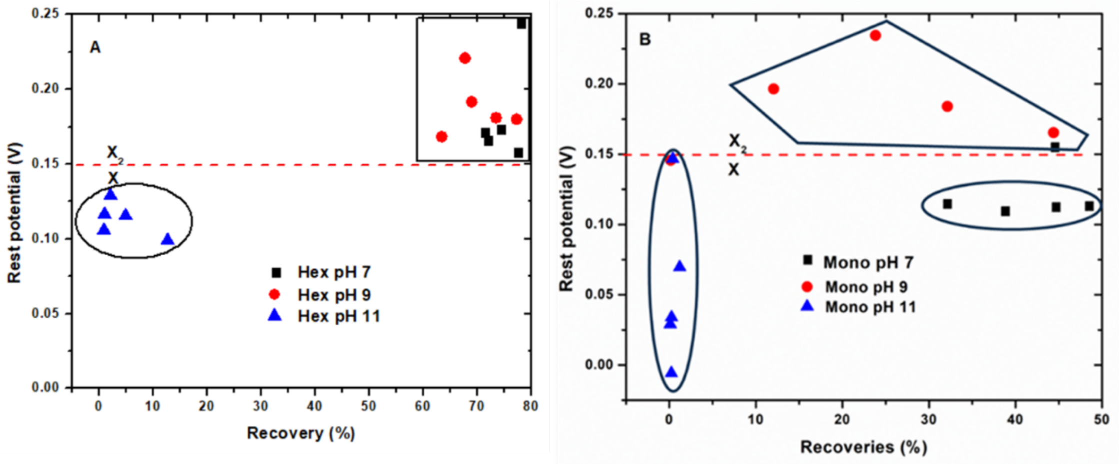

Fig. 12. Correlation between rest potential and flotation recovery for hexagonal and monoclinic pyrrhotite in the presence of xanthate collector, demonstrating how electrochemical conditions influence flotation efficiency across different pH levels and water chemistries

Fig. 12a displays a distinct increasing trend for hexagonal pyrrhotite: where elevated rest potentials were associated with enhanced recovery, especially as the potential neared or surpassed 0.15 V. This indicates that dixanthogen production was common and contributed to improved flotation, a result corroborated by the electrochemical evidence presented by Hodgson and Agar (1989) and the surface species model described by Yang et al. (2001). These studies established that under slightly oxidizing conditions, xanthate is oxidized into dixanthogen, which physisorbs onto pyrrhotite surfaces, creating a stable hydrophobic binding necessary for efficient flotation.

Conversely, the monoclinic pyrrhotite data depicted in Fig. 12b exhibits a more flat and irregular correlation. Despite rest potentials nearing 0.15 V at pH 7 and 9, the corresponding recoveries were low and inconsistent. This discrepancy may result from an increased propensity for surface passivation, leading to the formation of inactive surface precipitates that inhibit collector interaction. The passivating layers, consisting of compounds such as $Fe(OH)_3$ and sulphoxy complexes, may obstruct redox transitions at the mineral interface, hence restricting the formation of dixanthogen despite seemingly favorable rest potential conditions. This explains the variation in recovery despite comparable rest potential magnitudes relative to hexagonal pyrrhotite.

A notable observation from Fig. 12a is that at pH 11, the recovery of hexagonal pyrrhotite declined significantly, with all values remaining under 15%. The significant decrease indicates that elevated pH levels rendered the electrochemical conditions inadequate for dixanthogen formation (i.e., rest potential below 0.15 V), limiting surface interaction to the formation of metal xanthate. Due to the instability of metal xanthates and their susceptibility to desorption or oxidation in alkaline environments, the hydrophobic layer likely deteriorates, leading to poor flotation performance. Increased OH^- activity could also contribute this degradation since it helps to generate hydrophilic surface precipitates (such as $Fe(OH)_3$) that passivate the surface and restrict collector access. The results correlate with those of Wang and Peng (2014), who observed that surface coating and collector displacement often cause flotation to be hampered under high-pH and high- Ca^{2+} conditions. As no stable hydrophobic surface species exist at pH 11, in contrast to lower pH levels, the flotation recovery of hexagonal pyrrhotite suffered a significant decrease.

Overall, rest potential and microflotation results provide a means to show the intricate interaction among surface speciation, mineral structure, and solutions chemistry: Whereas monoclinic pyrrhotite showed reduced recovery due to kinetic and structural constraints, hexagonal pyrrhotite responded strongly to redox conditions favourable for dixanthogen formation. These results highlight a need for considering both mineralogy and water composition in flotation optimization since similar electrochemical potentials may produce different flotation responses dependent upon the structure-specific surface chemistry and reactivity.

4. Coupled roles of structure and ionic composition in pyrrhotite flotation

The collective results of this study converge on a unified mechanism that distinguishes how crystal structure governs pyrrhotite flotation under variable ionic conditions (Fig. 13). In pure water (Step one), both monoclinic and hexagonal pyrrhotite undergo oxidative dissolution ($Fe_{1-x}S + H_2O + O_2 \rightarrow Fe^{2+} + SO_4^{2-} + H^+$). However, monoclinic pyrrhotite exhibits higher reactivity, forming thicker hydrophilic layers of $Fe(OH)_x$, FeOOH, elemental sulfur, and polysulfides, which limit the availability of Fe–S sites. By contrast, hexagonal pyrrhotite experiences less extensive oxidation, retaining more electrochemically active Fe–S domains that remain favorable for collector interaction.

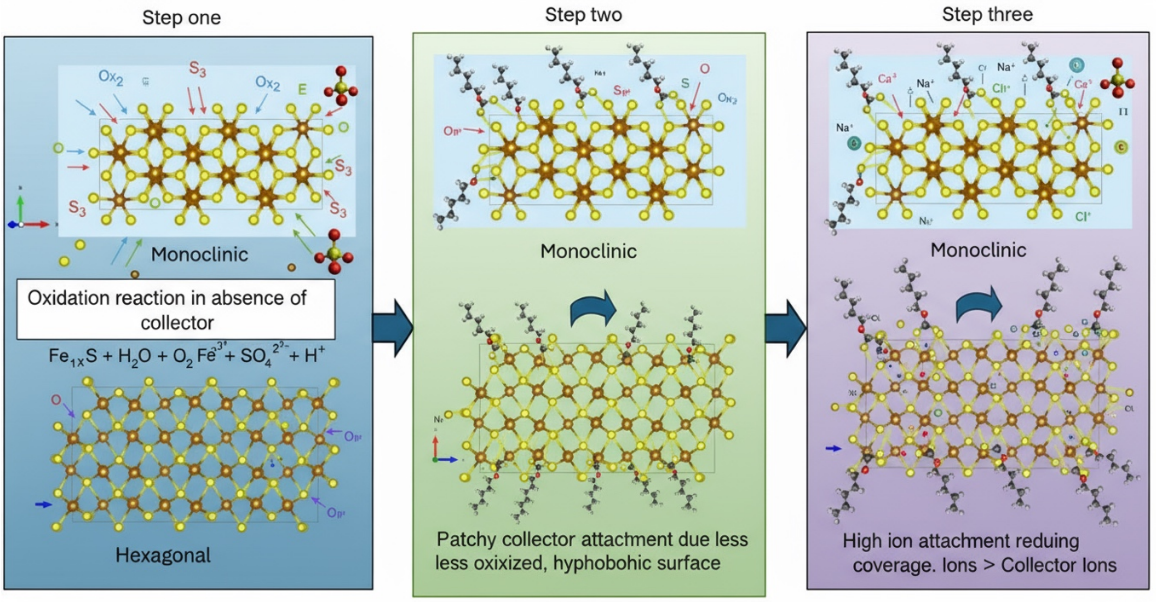

Fig. 13. Unified mechanism of pyrrhotite flotation in varying water chemistries

In the absence of dissolved ions (Step two), hexagonal pyrrhotite sustains broader xanthate coverage because its surface is less obstructed by hydrophilic phases. By contrast, adsorption on monoclinic pyrrhotite is spatially heterogeneous due to oxidation-derived passivation, which restricts the availability of binding sites. These findings are consistent with previous work showing that structural and electrochemical heterogeneity governs the probability of effective collector interaction (Janzen et al., 2000; Multani et al., 2018). When ions are introduced (Step three), the structural differences become amplified. Monoclinic pyrrhotite exhibits preferential uptake of Ca^{2+}, Na^+, Cl^-, and SO_4^{2-}, which form surface complexes that suppress hydrophobic film formation despite visible collector adsorption (Corin et al., 2011; Manono et al., 2012, 2016). Hexagonal pyrrhotite, by contrast, maintains a more negative zeta potential and adsorbs fewer ions, thereby sustaining higher effective collector coverage. This observation parallels results of October et al. (2021), who reported that electrostatic conditions in saline waters can favor attachment even when adsorption is limited, and aligns with reports of cation-driven passivation reducing flotation selectivity at alkaline pH (Kirjavainen et al., 2002; Musuku and Dahl, 2022). The integrated framework thus explains why monoclinic pyrrhotite frequently showed high collector uptake but low recovery, while hexagonal pyrrhotite achieved superior flotation despite comparable adsorption. The results demonstrate that the flotation response of pyrrhotite superstructures is governed not solely by the extent of collector adsorption, but by the interplay of structural reactivity, ion-specific interactions, and the persistence of electrochemically active Fe–S sites.

5. Conclusions

This study demonstrates the critical role of ionic composition in influencing the flotation behavior and surface electrochemistry of pyrrhotite superstructures, with a focus on the impact of ions such as Ca^{2+}, Na^+, Cl^-, SO_4^{2-}, and Mg^{2+}. By integrating microflotation, collector adsorption, zeta potential, and rest potential data, the study provides a comprehensive understanding of how surface charge, redox behavior, and reagent interaction work together under varied pH and ionic conditions. The following key conclusions can be drawn:

1. Hexagonal pyrrhotite consistently outperformed monoclinic pyrrhotite in flotation across all types of synthetic plant water. In contrast, monoclinic pyrrhotite showed greater sensitivity to rising ionic strength and pH levels, resulting in notable drops in recovery under conditions with high ionic concentrations.
2. Collector adsorption increased with ionic strength for both pyrrhotite types. However, hexagonal pyrrhotite showed a more robust and consistent adsorption profile, which better aligned with its flotation trends indicating a stronger affinity for collector molecules even under chemically challenging conditions.
3. Zeta potential measurements showed that increasing ionic strength compressed the electrical double layer, shifting surface charge toward less negative or near-neutral values. Hexagonal pyrrhotite exhibited greater responsiveness to these shifts, particularly at lower pH, while monoclinic pyrrhotite required more alkaline conditions for similar electrokinetic changes.
4. Rest potential data in the absence of collector indicated that hexagonal pyrrhotite maintained higher electrochemical nobility, suggesting reduced surface oxidation and better preservation of active sites. Monoclinic pyrrhotite displayed lower rest potentials under the same conditions, pointing to increased surface reactivity and passivation.
5. In the presence of collector, rest potentials enabled surface species identification, showing that hexagonal pyrrhotite was more likely to form hydrophobic dixanthogen at moderate pH and low ionic strength, while monoclinic pyrrhotite favored the formation of metal xanthate species, particularly in high-pH, high-ion waters.
6. The integrated analysis revealed that flotation performance was governed not just by collector adsorption, but by the alignment between surface charge and redox environment. Only when both were favorable i.e., adequate collector coverage and rest potentials in the dixanthogen-forming regime did flotation reach optimal levels.
7. While this study provided a first systematic evaluation of pyrrhotite superstructures under controlled ionic environments, future work should focus on isolating the role of individual ions and directly characterizing surface speciation. Advanced surface techniques such as SEM-EDS and XPS, coupled with DFT analysis, will be essential to quantify oxide and hydroxide layer formation, ion–collector competition, and the molecular-scale mechanisms that underpin the observed flotation behavior.

Overall, hexagonal pyrrhotite exhibited greater surface stability, adaptability, and hydrophobic layer-forming potential in complex water chemistries, reflecting greater challenge to depress using recycled or degraded water sources. Monoclinic pyrrhotite was far more sensitive to changes in pH and ionic composition. As a result, it showed a stronger tendency to be depressed under complex electrochemical conditions by the changes in the ionic strength of recycled water.

Acknowledgment

The authors would like to extend their heartfelt appreciation to NSERC Alliance and Mitacs Accelerate, in partnership with SK Godelius, Glencore Sudbury Integrated Nickel Operations, Vale, and Magotteaux, for their significant contribution. This support was instrumental in the successful completion of this research. The staff members at Queen's University's Robert M. Buchan Department of Mining and Department of Chemical Engineering are acknowledged for their consistent assistance, direction, and provision of necessary resources during the duration of this study.

References

BECKER, M., DE VILLIERS, J., BRADSHAW, D., 2010. *The flotation of magnetic and non-magnetic pyrrhotite from selected nickel ore deposits.* Minerals Engineering, 23(12), 1045–1052.

BELZILE, N., CHEN, Y.W., CAI, M.F., LI, Y., 2004. *A review on pyrrhotite oxidation.* Journal of Geochemical Exploration, 84(1–3), 65–76.

BOUJOUNOUI, K., ABIDI, A., BACAOUI, A., EL AMARI, K., YAACOUBI, A., 2015. *The influence of water quality on the flotation performance of complex sulphide ores: Case study at Hajar Mine, Morocco.* Journal of the Southern African Institute of Mining and Metallurgy, 115(12), 1243–1251.

BUSWELL, A.M., NICOL, M.J., 2002. *Some aspects of the electrochemistry of the flotation of pyrrhotite.* Journal of Applied Electrochemistry, 32(12), 1321–1329.

CHENG, X., 1993. *Electrochemical characteristics of pyrrhotite and its implication to flotation* (Doctoral dissertation, University of Minnesota).

CHO, Y.S., LASKOWSKI, J.S., 2002. *Effect of flotation frothers on bubble size and foam stability.* International Journal of Mineral Processing, 64, 69–80.

CORIN, K.C., REDDY, A., MIYEN, L., WIESE, J.G., HARRIS, P.J., 2011. *The effect of ionic strength of plant water on valuable mineral and gangue recovery in a platinum-bearing ore from the Merensky reef.* Minerals Engineering, 24, 131–137.

CRAIG, V., NINHAM, B., PASHLEY, R., 1993. *The effect of electrolytes on bubble coalescence in water.* Journal of Physical Chemistry, 39, 10192–10197.

DAVIS, F., HYATT, D., COX, C., 1975. *Environmental problems of flotation reagents in mineral processing plant tailings water.* U.S. Department of the Interior, Washington, DC, USA.

EKMEKÇI, Z., BECKER, M., BAGCI TEKES, E., BRADSHAW, D., 2010. *The relationship between the electrochemical, mineralogical and flotation characteristics of pyrrhotite samples from different Ni ores.* Journal of Electroanalytical Chemistry, 647, 133–143.

HODGSON, M., AGAR, G.E., 1989. *Electrochemical investigations into the flotation chemistry of pentlandite and pyrrhotite: Process water and xanthate interactions.* Canadian Metallurgical Quarterly, 28(3), 189–198.

IKUMAPAYI, F., MAKITALO, M., JOHANSSON, B., RAO, K.H., 2014. *Recycling of process water in sulphide flotation: Effect of calcium and sulphate ions on flotation of galena.* Proceedings of the XXVII International Mineral Processing Congress, Cape Town, South Africa.

JANZEN, M.P., NICHOLSON, R.V., SCHARER, J.M., 2000. *Pyrrhotite reaction kinetics: Reaction rates for oxidation by oxygen, ferric iron, and for nonoxidative dissolution.* Geochimica et Cosmochimica Acta, 64(9), 1511–1522.

KIRJAVAINEN, V., SCHREITHOFER, N., HEISKANEN, K., 2002. *Effect of calcium and thiosulfate ions on flotation selectivity of nickel–copper ores.* Minerals Engineering, 15(1), 1–5.

LASKOWSKI, J.S., 2013. *From amine molecules adsorption to amine precipitate transport by bubbles: A potash ore flotation mechanism.* Minerals Engineering, 45, 170–179.

LASKOWSKI, J.S., CASTRO, S., 2017. *Hydrolysis of metallic ions in mineral processing circuits and its effect on flotation.* Proceedings of the COM Conference of Metallurgists, Vancouver, BC, Canada, 27–30 August.

LEVAY, G., SMART, R., SKINNER, W., 2001. *The impact of water quality on flotation performance.* Journal of the Southern African Institute of Mining and Metallurgy, 1, 69–76.

MANONO, M.S., CORIN, K.C., WIESE, J.G., 2012. *An investigation into the effect of various ions and their ionic strength on the flotation performance of a platinum-bearing ore from the Merensky reef.* Minerals Engineering, 36–38, 231–236.

MANONO, M.S., CORIN, K.C., WIESE, J.G., 2016. *The influence of electrolytes present in process water on the flotation behaviour of a Cu-Ni containing ore.* Minerals Engineering, 96–97, 85–93.

MANONO, M., CORIN, K., WIESE, J., 2018. *Perspectives from literature on the influence of inorganic electrolytes present in plant water on flotation performance.* Physicochemical Problems of Mineral Processing, 54, 1191–1214.

MOIGNARD, M.S., JAMES, R.O., HEALY, T.W., 1977. *Adsorption of calcium at the zinc sulphide–water interface.* Australian Journal of Chemistry, 30, 733–740.

MULTANI, R.S., WILLIAMS, H., JOHNSON, B., LI, R., WATERS, K.E., 2018. *The effect of superstructure on the zeta potential, xanthate adsorption, and flotation response of pyrrhotite.* Colloids and Surfaces A: Physicochemical and Engineering Aspects, 555, 72–81.

MUSUKU, B., DAHL, O., 2022. *Impact of recycled process water on electrochemical reactivity of sulphide ore.* Minerals, 12(11), 1455.

MUZENDA, E., 2010. *An investigation into the effect of water quality on flotation performance.* World Academy of Science, Engineering and Technology, 70, 237–241.

MUZINDA, I., SCHREITHOFER, N., 2018. *Water quality effects on flotation: Impacts and control of residual xanthates.* Minerals Engineering, 125, 34–41.

Supplementary data

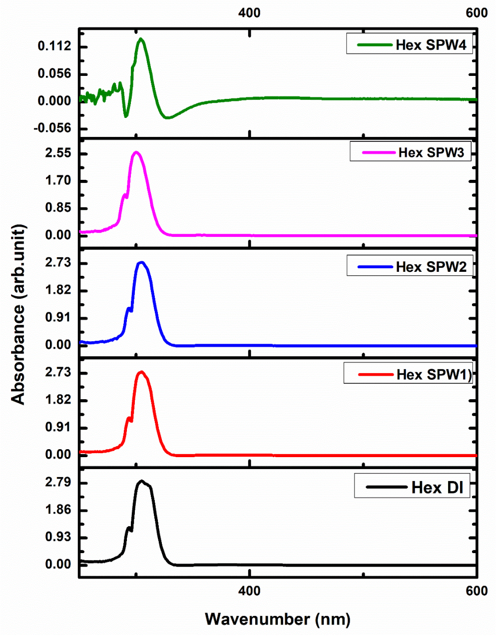

Fig. 1. UV-vis spectra of the supernatant from conditioning of hexagonal at pH 9

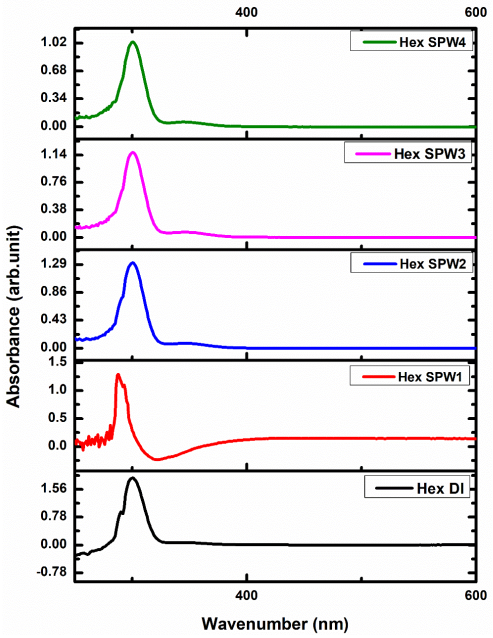

Fig. 2. UV-vis spectra of the supernatant from conditioning of hexagonal at pH 11

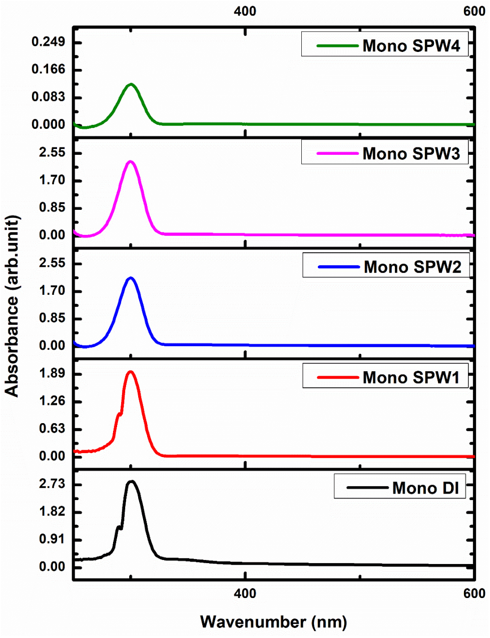

Fig. 3. UV-vis spectra of the supernatant from conditioning of Monoclinic at pH 7

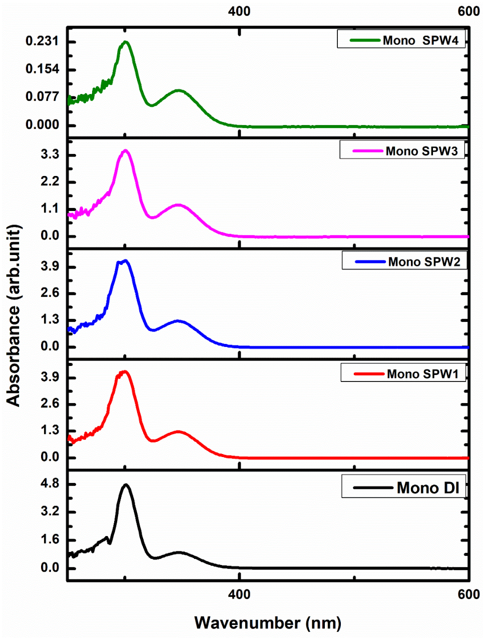

Fig. 4. UV-vis spectra of the supernatant from conditioning of Monoclinic at pH 9